Journal of Atmospheric and Terrestrial Physics, Vol. 43, No. 4, pp. 345–354, 1981.
Printed in Northern Ireland

0021-9169/81/040345-08$02.00/0
Pergamon Press Ltd.

Atomic oxygen determination from a nitric oxide point release in the equatorial lower thermosphere

E. VAN HEMELRIJCK
Belgian Space Aeronomy Institute, 3, Avenue Circulaire, B-1180 Bruxelles, Belgium

(*Received in final form* 17 *December* 1980)

Abstract—Atomic oxygen density values in the 80–105 km altitude equatorial region have been obtained by analyzing the chemiluminescence of nitric oxide point releases from three CENTAURE II-C rockets. The light emission produced by the NO—O chemiluminous recombination was sufficiently high to render the artificial clouds observable only by ground-based instruments. The difficulties associated with these kind of experiments have been greatly avoided by a new technique ejecting the NO gas into the backward direction of the flight. It has been found that below 90 km the derived atomic oxygen densities are in relatively good agreement with those reported by other workers. At approximately 105 km the measured value is about two times higher than the $n(O)$ density obtained by averaging a set of data from a great number of other flights but coincides rather well with the measurements of DICKINSON *et al.* (1980).

1. INTRODUCTION

In situ measurements of the composition and structure of the lower thermosphere are scarce and often incomplete. On one hand, the perigee of an artificial satellite is generally located above an altitude of approximately 150 km and, on the other hand, the cumulation altitude of rockets of the meteorological type do not exceed a height of about 60 km. The observations are still more reduced if one considers only those dealing with atomic oxygen. Nevertheless, several methods have been developed to determine its concentration as a function of altitude.

Experimentally its distribution has been measured principally by mass spectrometric techniques (OFFERMANN and DRESCHER, 1973; PHILBRICK *et al.*, 1973, 1977; KRANKOWSKY *et al.*, 1977; TRINKS *et al.*, 1978) and by using photometry of green line (557.7 nm) intensity from airglow emission (TARASOVA, 1963; O'BRIEN *et al.*, 1965; BAKER and WADDOUPS, 1967, 1968; GULLEDGE *et al.*, 1968; DANDEKAR and TURTLE, 1971; DANDEKAR, 1972; OFFERMANN and DRESCHER, 1973; KULKARNI, 1976).

In the past ten years new experimental methods have been successfully demonstrated: the silver film oxidation method (HENDERSON and SCHIFF, 1970; HENDERSON, 1971, 1974), the measuring of the infrared bands of the excited hydroxyl radical in the night airglow (GOOD, 1976), catalytic probes (PEROV and RAKHMANOV, 1975, 1976) and rocket borne OI resonance-scattering systems (DICKINSON *et al.*, 1974, 1976, 1980; HOWLETT *et al.*, 1980). An indirect method has been suggested by ZALPURI and OGAWA (1979) for deriving the density profile from positive ion composition data as observed from mass spectrometric experiments.

Although those new methods give relatively good results it must be pointed out that most of them are still in a developmental stage and that mainly instrumental improvements are necessary in order to obtain greater accuracies and higher reliabilities indispensable to the study of the composition of the lower thermosphere.

Finally, the atomic oxygen number density can be derived from the well known nitric oxide release method (PRESSMAN *et al.*, 1956; GOLOMB *et al.*, 1965; SPINDLER, 1966; GOLOMB and GOOD, 1966, 1972; GOOD and GOLOMB, 1973; ARMSTRONG *et al.*, 1975), based on the measurement of the light intensity radiated by a NO release from a rocket at night in the 80–140 km region of the atmosphere.

In spite of some difficulties associated with this experimental technique the main advantages are that only a simple payload is required (a tankful of compressed nitric oxide, a timer and an opening system) and that all the observations may be realised by ground-based photographic instruments.

From an analysis of all reported nitric oxide releases it may be concluded that this experimental technique is a very useful research tool if the following conditions are satisfied:

(a) the hydrodynamical picture of the gas release has to present a simple form easy to evaluate;

(b) the reaction rate constants for the NO—O chemiluminescent recombination have to be known with sufficient accuracy;

(c) an accurate knowledge of the reaction mechanism leading to the formation of the NO_2 molecule is required.

Our experiment differed from previous ones by using point releases and by ejecting the NO gas into the backward direction of the flight.

2. EXPERIMENT

Three experiments have been realised, code named NO-II-1, NO-II-2 and NO-II-3. The payloads were brought to altitude by CENTAURE II-C rockets launched from Kourou, French Guyana (5.2°N, 52.8°W) on 12 September 1974 (two rockets), at 2220 UT and 2326 UT respectively, and on 13 September 1974 at 2223 UT.

The scientific experiment consisted of a four-fold nitric oxide release at four different altitudes in the 80–105 km region.

Each payload included mainly a mechanical structure with four bottles containing the gas, a radar transponder, a timer, a security box, explosive actuated miniature switches, batteries and a pyrotechnic system to open the bottles. More experimental details are given by FRIMOUT *et al.* (1975) and in Fig. 1.

2.1. *Gas release*

The nitric oxide was contained in a four liter cylindrical aluminium container made of a monoblock bulk without welding joints and manufactured by the Société Métallurgique de Gerzat (France). The gas was at 50 atm, the total amount of the released gas being 268 g per bottle corresponding to approximately 5.4×10^{24} molecules.

To satisfy the first condition mentioned in the introduction we decided to use a point release in order to obtain a quasi-spherical artificial cloud. The pyrotechnic system, fixed at the bottom of each NO container, was constructed by the Poudreries Réunies de Belgique. Filled with a 6.8 g explosive charge, the pyrotechnics were capable of making a hole in the bottles of about 40 mm in diameter. Theoretical analysis, confirmed by ground experiments showed that, at altitudes between 80 and 105 km, 99% of the total amount of gas was ejected into the rarefied atmosphere in less than 0.07 s.

Furthermore, the difficulties with the gasdynamic model have been greatly avoided by releasing the NO-jet into the backward direction of the flight; as a result, the absolute speed of the flow remains subsonic without the creation of a shock wave. To the best of our knowledge a similar technique has not yet been applied. This improvement, as well as the use of a point release, facilitates considerably the determination of the reaction volume and of the partial density of nitric oxide.

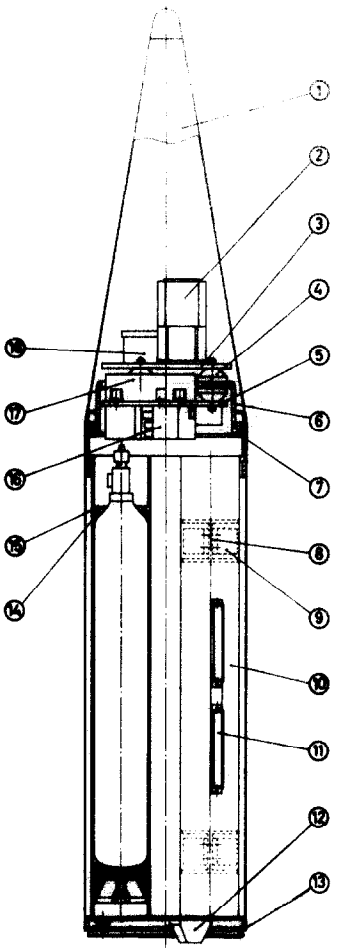

Fig. 1. Schematic view of the NO-II payload. 1. Nose cone. 2. Security box. 3. Upper plate. 4. Shock mount. 5. Lower plate. 6. Intermediary plate. 7. Upper bulkhead. 8 and 9. Attachment ring. 10. Cylindrical pipes for the mounting of the bottles. 11. Explosive actuated miniature switch. 12. Mechanical stop unit for the preloaded spring system. 13. Lower bulkhead housing two manacle units. 14. Rubber seal (O-ring). 15. Stop flange ring. 16. Batteries. 17. Timer. 18. Radar transponder. The pyrotechnic devices used to make a hole in the bottles are fixed at the bottom of each cylinder.

The releases were made at four intervals: the first starting at $H_0 + 82$ s (H_0 being the time of lift-off of the rocket), the latest taking place at $H_0 + 112$ s.

Two identical but independent timing circuits were used; a high degree of reliability was thus guaranteed. Each time circuit consisted of an

Table 1. Optical characteristics of the main ground-based observational instruments

Instrument	Lens opening	Focal length (mm)	Film or plate	Field of view	Exposure time
Gianini camera	*f*/0.87	77	Kodak 2485 (35 mm)	18×26°	2 or 5s
IAS triangulation camera	*f*/5	500	Kodak 103F (200×250 mm)	22×28°	5 min
Television camera	*f*/4.5	500		5°	50 frames per second
Huet spectrograph	*f*/0.7	600	Kodak 103F (45×60 mm)	≈6°	

ignitor firing battery, current limiting resistors, ignitors and a receptacle for safe, test and arming plugs.

The payload was brought to altitude by a two stage solid propellant CENTAURE II-C rocket, the second stage burning out at an altitude of about 25 km. The two manacle rings were jettisoned at approximately 65 km; at the same time the preloaded spring system separated the payload from the CENTAURE II-C rocket with a speed of more than 2 ms^{-1}.

2.2. *Ground-based observational instruments*

The main ground-based instruments, located at four observation sites, for the measurements of atomic oxygen density, precise altitude of the artificial clouds and the wind speed at the release heights were the following: two Gianini cameras (Van Hemelrijck, 1981a,b), two IAS triangulation cameras (Debehogne *et al.*, 1976), two Westinghouse TV cameras (Debehogne and Van Hemelrijck, 1977) and one Huet type CI spectrograph. Some characteristic features of these instruments are listed in Table 1.

It should be noted that the Huet spectrometer, with a spectral range from 380 to 650 nm, was a manually guided instrument. Due to the narrow field of view and to the relatively small light emission of the artificial clouds, no spectra of the NO—O chemiluminescent reaction could be detected. Therefore, previously determined emission spectra mainly obtained by laboratory experiments (Fontijn and Schiff, 1961; Fontijn *et al.*, 1964; Good, 1967; Paulsen *et al.*, 1970; Golomb and Brown, 1975) have been taken into account for the data reduction.

3. DETERMINATION OF ATOMIC OXYGEN CONCENTRATION

The usual schematic reaction mechanism for the NO—O chemiluminous recombination is (Golomb and Brown, 1975):

$$(k_1);\ NO + O + M \rightarrow NO_2^* + M \quad (1)$$

$$(k_R);\ NO_2^* \rightarrow NO_2 + h\nu \quad (2)$$

and

$$(k_Q);\ NO_2^* + M \rightarrow NO_2 + M. \quad (3)$$

Steady state treatment of the reactions (1), (2) and (3) leads to:

$$I = \frac{k_1 n(NO) n(O) n(M)}{1 + [k_Q n(M)/k_R]} \approx I_0^a n(NO) n(O) \quad (4)$$

where $I_0^a = k_1 k_R k_Q^{-1}$ is the photon emission rate coefficient ($cm^3\ s^{-1}$) and I is the total number of photons (photons $cm^{-3}\ s^{-1}$) emitted per unit time and per unit volume.

According to Golomb and Brown (1975) the best fit expression for the photon emission rate coefficient is given by:

$$I_0^a = (1.15 \pm 0.1) \times 10^{-17} (300/T)^{0.9} \exp(350/T) (cm^3\ s^{-1}) \quad (5)$$

which is applicable to the 170–1250 K and 400–800 nm range. In our calculations the temperature T has been taken from the U.S. Standard Atmosphere Supplements, 1966.

Finally, atomic oxygen concentration is given by:

$$n(O) = I/[I_0^a n(NO)] \quad (6)$$

where I is the observed photon emission rate.

In the gas release technique used by Golomb *et al.* (1965) it was necessary to take into account the mixing layer between the inner shock and the bow shock. The present experiment was performed without creation of a shock wave. It is, therefore, reasonable to assume that nitric oxide diffuses spherically according to a Gaussian law. The radius of the cloud varies with time and the concentration of NO is obtained from the knowledge of the emitting volume as a function of time, since the

ejected amount of NO is known. The mean radius of the artificial cloud is calculated by means of a Joyce and Loebl double-beam recording isodensitometer.

The total quantity of light energy deposited on the Gianini-films was determined from isodensity traces of the photographs and by means of relative and absolute calibrations (VANDEN BORRE, 1975).

A detailed description of the procedure to convert this energy into the total number of photons I ($h\nu$ cm^{-3} s^{-1}) emitted by the artificial clouds is given in the appendix; the derived expression of I can be written in the following form:

$$I = 5.907\times10^{-19}[r_e^2 L(0) S_R^2/Vt] \times \sum_{i=1}^{13} [P_i\varepsilon_i/T(A)_i T(G)_i](h\nu \text{ cm}^{-3}\text{ s}^{-1}) \quad (7)$$

where

r_e = Gaussian half-width, i.e. the distance on the densitometric recording image at which the radiant exposure is $1/e$ times the peak value;

$L(0)$ = radiance in the center of the image:

S_R = slant-path, i.e. the distance between the camera and the artificial cloud;

V = reaction volume of nitric oxide;

t = exposure time of the film;

ε_i = energy conversion factor ($J \rightarrow h\nu$) for the ith wavelength interval ($i = 1, \ldots, 13$);

$T(A)_i$ = atmospheric transmission coefficient from sea level to space;

$T(G)_i$ = camera lens transmission coefficient;

E_i = relative luminous intensity of the emitted NO—O spectrum;

S_i = adopted relative spectral sensitivity of the film;

$P_i = E_i S_i / \Sigma E_i S_i$.

4. OBSERVATIONS

As already mentioned, the three payloads consisted each of four cylinders, filled with compressed nitric oxide, to be opened at four different altitudes between 80 and 105 km. As a result, twelve releases had to take place; unfortunately, only six artificial clouds were observed.

Table 2 represents the launch times of the NO-II experiment and also the number of observed artificial clouds, while Figs. 2 and 3 give respectively a photograph of the nitric oxide point releases of the NO-II-3 experiment and a magnification of some typical isodensitometric images.

Table 2. Launch time and number of observed artificial clouds for the NO-II release experiment

Code name	Date	Launch time (UT)	Observed Clouds
NO-II-1	12 Sept. 1974	22:20:32	1–2
NO-II-2	12 Sept. 1974	23:26:19	1
NO-II-3	13 Sept. 1974	22:23:05	1–2–3

It should be noted that the NO-II-2-1 release yielded only one determination of n(O). The ejection altitude being 80.7 km, the measured atomic oxygen concentration was so low (2.1×10^{10} cm^{-3}) that the luminous intensity of the chemiluminous NO—O reaction could only be observed on one photograph taken by the Gianini cameras. The total number of photons emitted was equal to 1.03×10^{8} h cm^{-3} s^{-1} corresponding to a global emission rate of 1.63×10^{5} rayleigh or to a power emitted of approximately 5 W; for comparison, typical radiant flux values for the other releases ranged from 100 to 200 W.

5. RESULTS AND DISCUSSION

Resulting atomic oxygen densities as calculated from expression (6) are plotted in Figs. 4 and 5. The data are obtained from 66 isodensity traces of 2 or 5 s exposure photographs and represent averages over two observation sites.

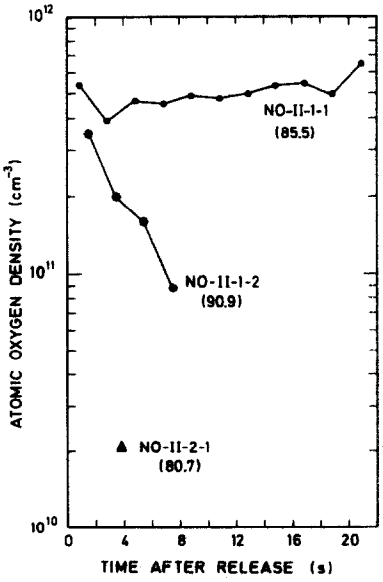

Fig. 4. Distribution of atomic oxygen density versus time after release for the two flights of 12 September 1974. The corresponding altitudes are given in parenthesis.

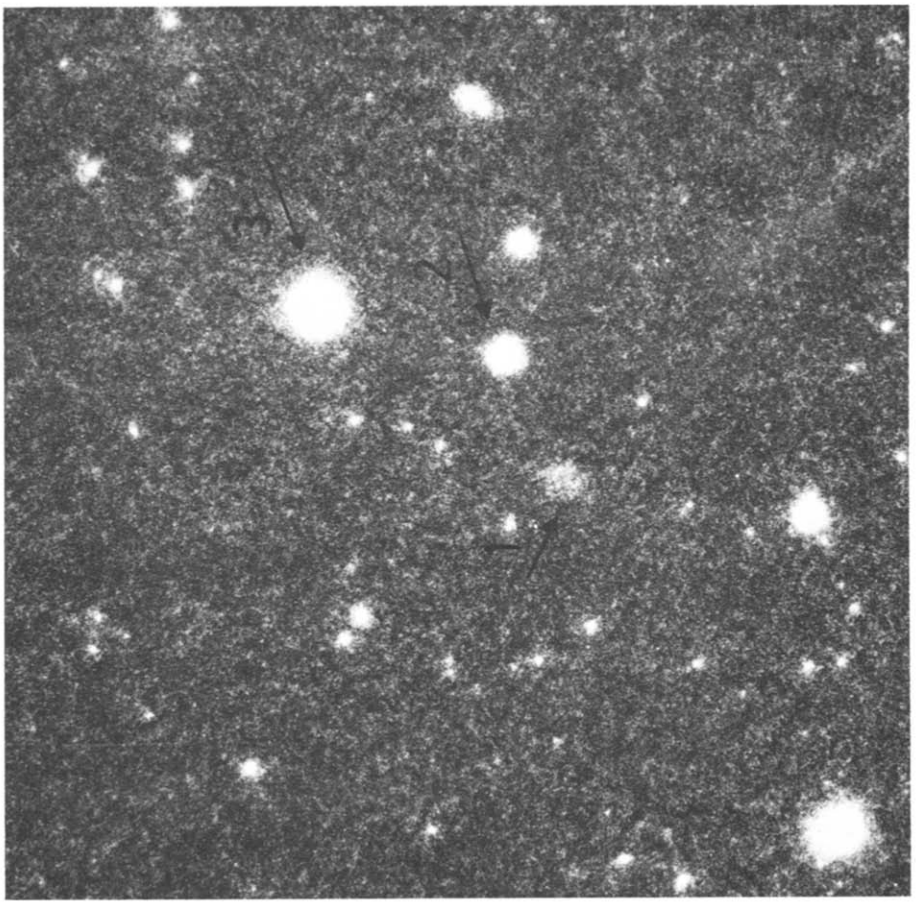

Fig. 2. Five-second exposure photograph of the nitric oxide point releases (NO-II-3). Note also the presence of stars under the form of luminous spots.

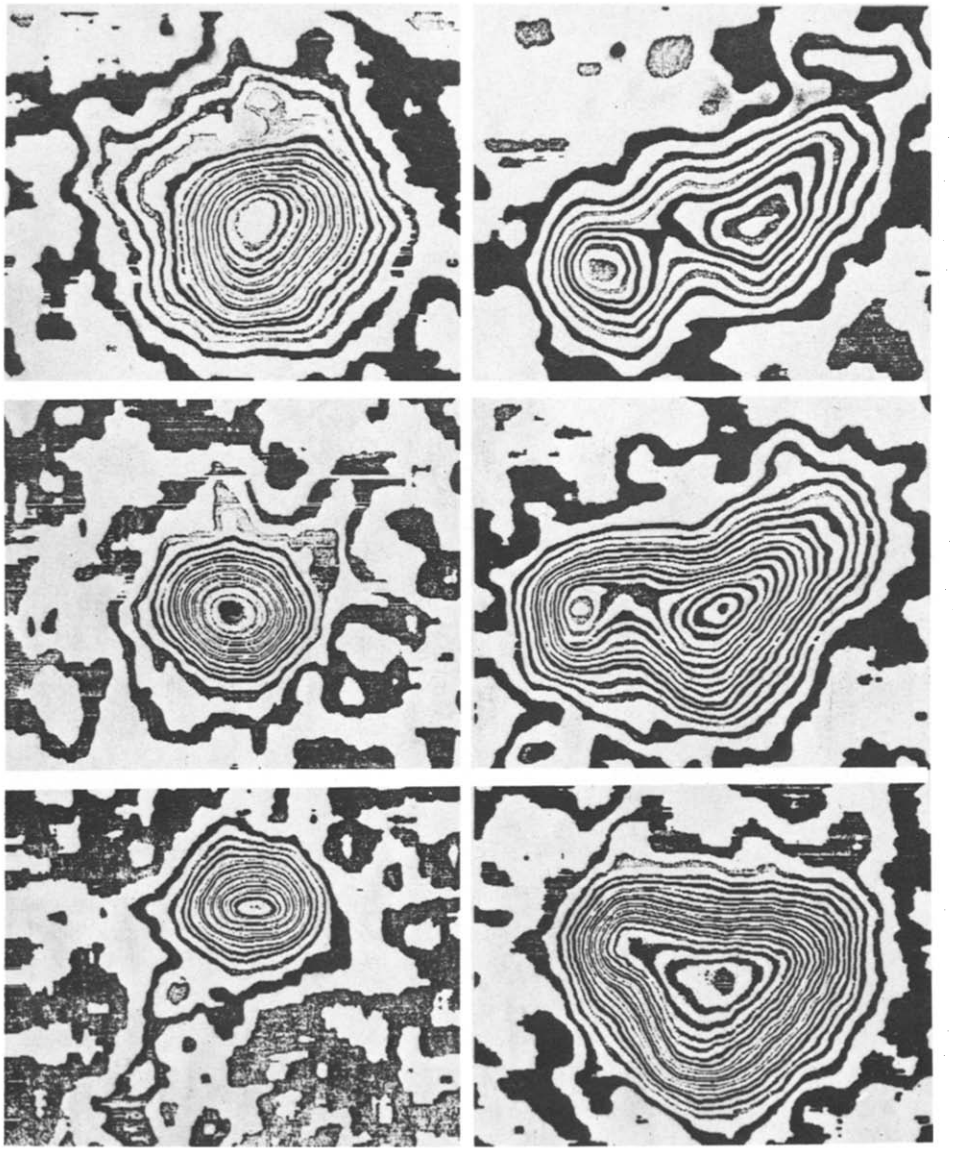

Fig. 3. Some typical concentric isocontours of the artificial clouds of the NO-II-3 experiment. a. First cloud. H (release time) = 22:24:28. b. Second cloud. H = 22:24:33. c, d, e and f. Third cloud. H = 22:24:50, H + 15s, H + 30s, H + 45s.

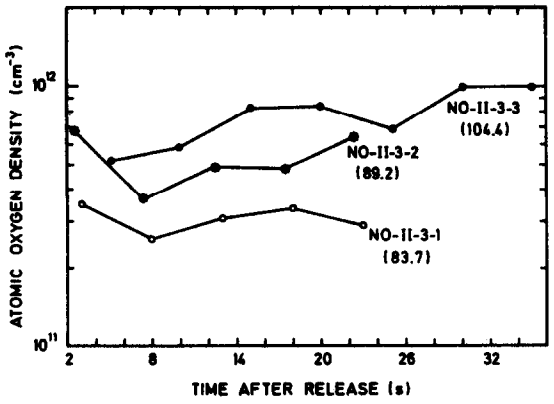

Fig. 5. Distribution of atomic oxygen density versus time after release for the flight of 13 September 1974.

A calculated uncertainty level of the $n(O)$ values, based on an error analysis of each measurement, was assumed to be ±30%. However, the estimation of the error bar is rather difficult due to the fact that the final determination of $n(O)$ depends on several parameters. The uncertainty in the derived atomic oxygen density is mainly caused by the limitation on accuracy of the optical film densities and of the photon emission rate coefficient $I_0{}^a$.

An analysis of the results (Figs. 4 and 5) indicates that the atomic oxygen concentration as a function of time after release remains relatively constant, except for the NO-II-1-2 release where the observed number density decreases by a factor of 4 in a very short time interval (8 s). This sharp decrease is caused by a sudden decrease of the total number of photons emitted. The reason for this phenomenon is not very clear.

Our results are compared with nighttime number densities, covering the 80–110 km altitude span, reported by other workers as illustrated in Fig. 6. A mean curve (solid trace) was drawn through 5 km interval data points, the NO-II values (dashed curve) representing the arithmetic averages of all measurements made at a given altitude. It should be noted that only the largest 90.9 km density was retained, the resulting $n(O)$ value being the most realistic.

Such a comparison gives only a qualitative idea about the density distribution since, on one hand, the atomic oxygen profile often shows a rather complex structure and, on the other hand, the number density is a function of local time, latitude and season. Furthermore, the data points available in the lower thermosphere, especially below 90 km, are scarce. It follows that the spread in measured values is sometimes greater than one order of magnitude.

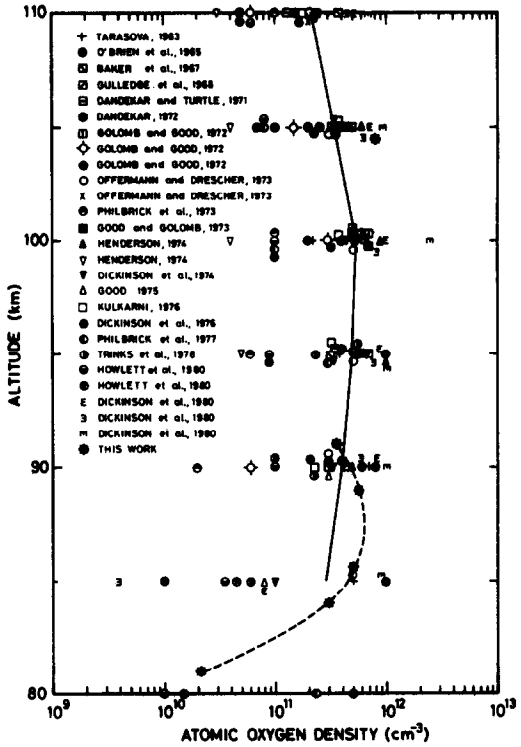

Fig. 6. Atomic oxygen density values as a function of altitude for Kourou (dashed curve) compared with number densities reported by other workers. The solid trace represents the mean curve drawn through 5 km interval data points; the NO-II values are the arithmetic averages of all measurements made at a given altitude.

The 85–90 km altitude range is the region where diurnal variation of $n(O)$ is expected to be minimum (Ogawa and Shimazaki, 1975; Zalpuri and Ogawa, 1979) and hence, any difference in most of the reported values shown in Fig. 6 may be due to seasonal and latitudinal change and, of course, to the uncertainty level of the measuring technique.

Figure 6 reveals that below approximately 90 km our derived NO-II atomic oxygen densities are in relatively good agreement with those obtained by other workers and that the deviations appear to be within the natural variability of the atmosphere. At about 105 km the derived value is more than two times higher than the $n(O)$ density obtained by averaging a set of data from a great number of other flights but coincides remarkably well with the values recently published by Dickinson *et al.* (1980).

It should be emphasized that most of the atomic oxygen densities reported to date are sampled at northern latitudes from 20 to 60°, but with a bias

towards the mid-latitudes. To the best of our knowledge only two experiments have been realised at equatorial latitudes i.e. KULKARNI (1976) on February 1973 from Thumba, India (8°33'N) and VAN HEMELRIJCK (this work) from Kourou, French Guyana (5°12'N).

By analyzing available data from 18 rocket experiments (OFFERMANN and DRESCHER, 1973) and by making a compilation of all reported nitric oxide releases and some mass-spectrometric measurements (GOOD and GOLOMB, 1973) it may be concluded that the mean height of maximum atomic oxygen number density is situated between 95 and 100 km. Although not enough statistical evidence is present to determine this peak altitude versus latitude there seems to be an indication of a possible increase of this height with decreasing latitude (KULKARNI, 1976 and this work). Contrary to the conclusion of KULKARNI (1976) that the density of atomic oxygen decreases with latitude with a minimum on the magnetic equator we found rather relative high values during the NO-II experiment.

Acknowledgements—The author would like to thank Dr. G. KOCKARTS for his careful reading of the manuscript and for his valuable comments in evaluating this paper.

The assistance of the technical staff of the Belgian Space Aeronomy Institute is very much appreciated and financial support was received from the Nationaal Fonds voor Wetenschappelijk Onderzoek.

REFERENCES

ARMSTRONG R. J., MASEIDE K. and TRØIM, J.	1975	*J. atmos. terr. Phys.* **37,** 797.
BAKER D. J. and WADDOUPS R. O.	1967	*J. geophys. Res.* **72,** 4881.
BAKER D. J. and WADDOUPS R. O.	1968	*J. geophys. Res.* **73,** 2546.
DANDEKAR B. S.	1972	*Planet. Space Sci.* **20,** 1781.
DANDEKAR B. S. and TURTLE J. P.	1971	*Planet. Space Sci.* **19,** 149.
DEBEHOGNE H., LIPPENS C., VAN HEMELRIJCK E. and VAN RANSBEECK E.	1976	*Annls. Géophys.* **32,** 195.
DEBEHOGNE H. and VAN HEMELRIJCK E.	1977	*Astron. and Astrophys.* **54,** 273.
DICKINSON, P. H. G., BOLDEN R. C. and YOUNG R. A.	1974	*Nature, Lond.* **252,** 289.
DICKINSON P. H. G., TWIDDY N. D. and YOUNG R. A.	1976	*Space Res.* **16,** 301.
DICKINSON P. H. G., BAIN W. C., THOMAS L., WILLIAMS E. R., JENKINS D. B. and TWIDDY N. D.	1980	*Proc. R. Soc. Lond., A* **369,** 379.
ELTERMAN L.	1964	*Appl. Optics* **3,** 1139.
ELTERMAN L.	1968	AFCRL-68-0153, Environmental Research Papers, 285.
FONTIJN A., MEYER C. B. and SCHIFF H. I.	1964	*J. chem. Phys.* **40,** 64.
FONTIJN A. and SCHIFF H. I.	1961	*Chemical reactions in the lower and upper atmosphere,* Interscience, New York, p. 239.
GOLOMB D. and BROWN J. H.	1975	*J. chem. Phys.* **63,** 5246.
GOLOMB D. and GOOD R. E.	1966	*J. geophys. Res.* **71,** 5753.
GOLOMB D. and GOOD R. E.	1972	*Space Res.* **12,** 1972.
GOLOMB D., ROSENBERG N. W., AHARONIAN C., HILL J. A. F. and ALDEN H. L.	1965	*J. geophys. Res.* **70,** 1155.
GOOD R. E.	1976	*Planet. Space Sci.* **24,** 389.
GOOD R. E. and GOLOMB D.	1973	*Space Res.* **13,** 249.
GULLEDGE I. S., PACKER D. M., TILFORD S. G. and VANDERSLICE J. T.	1968	*J. geophys. Res.* **73,** 5535.
HENDERSON W. R.	1971	*J. geophys. Res.* **76,** 3166.
HENDERSON W. R.	1974	*J. geophys. Res.* **79,** 3819.
HENDERSON W. R. and SCHIFF H. I.	1970	*Planet. Space Sci.* **18,** 1527.
HOWLETT L. C., BAKER K. D., MEGILL L. R., SHAW A. W., PENDLETON W. R. and ULWICK J. C.	1980	*J. geophys. Res.* **85,** 1291.
KULKARNI P. V.	1976	*J. geophys. Res.* **81,** 3740.
O'BRIEN B. J., ALLUM F. B. and GOLDWIRE H. C.	1965	*J. geophys. Res.* **70,** 161.
OFFERMANN D. and DRESCHER A.	1973	*J. geophys. Res.* **78,** 6690.
OGAWA T. and SHIMAZAKI T.	1975	*J. geophys. Res.* **80,** 3945.
PAULSEN D. E., SHERIDAN W. F. and HUFFMAN R. E.	1970	*J. chem. Phys.* **53,** 647.
PEROV S. P. and RAKHMANOV A. S.	1976	*Space Res.* **17,** 261.
PHILBRICK C. R., FAUCHER G. A. and TRZCINSKI E.	1973	*Space Res.* **13,** 255.
PHILBRICK C. B., FAUCHER G. A. and BENCH P.	1977	*Space Res.* **18,** 139.

PRESSMAN J., ASCHENBRAND L. M., MARMO F. F., JURSA A. and ZELIKOFF M.	1956	*J. chem. Phys.* **25,** 187.
SPINDLER G. B.	1966	*Planet. Space Sci.* **14,** 53.
TARASOVA T. M.	1963	*Space Res.* **3,** 162.
TRINKS H., OFFERMANN D., VON ZAHN U. and STEINHAUER C.	1978	*J. geophys. Res.* **83,** 2169.
VAN HEMELRIJCK E.	1981a	Accepted in *Annls Géophys.*, 1980.
VAN HEMELRIJCK E.	1981b	*Ciel et Terre,* **96,** 135.
ZALPURI K. S. and OGAWA T.	1979	*J. atmos. terr. Phys.* **41,** 961.

Reference is also made to the following unpublished material

FRIMOUT D., LIPPENS C., SIMON P., VAN HEMELRIJCK E. and VAN RANSBEECK E.	1975	Proceedings of the Colloque International: Technologie des expériences scientifiques spatiales, p. 569.
GOOD R. E.	1967	AFRCL 67-0193.
KRANKOWSKY D., ARNOLD F., FRIEDRICH V. and OFFERMANN D.	1977	Paper presented at the COSPAR 20th General Assembly, Tel Aviv, Israel.
PEROV S. P. and RAKHMANOV A. S.	1975	Paper presented at the COSPAR 18th General Assembly, Varna, Bulgaria.
VANDEN BORRE C.	1975	Dissertation, Institut des Sciences Nucléaires Appliquées, Brussels.

APPENDIX. DETERMINATION OF THE TOTAL NUMBER OF PHOTONS I EMITTED

The J-L isodensitracer gives a set of concentric isocontours (Fig. 3) corresponding to a known optical density interval determined by the calibration of the instrument. The isodensitometric images have been analysed according to four axes, the center of the artificial clouds being taken as the origin.

Measurements of the characteristic curves (optical density versus radiant exposure in arbitrary units) of the Kodak 2485 films lead to the radiant exposure as a function of the distance from the center of each film (Fig. A.1, solid curve). This curve is compared with a best-fitted Gaussian density distribution (dashed curve) representing quantitatively the light energy deposited on the film during a time interval equal to the exposure time.

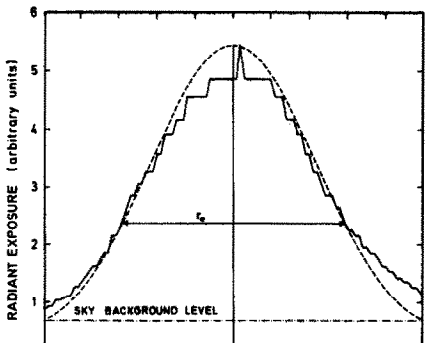

Fig. A.1. Typical plot of the radiant exposure in function of the distance from the center of the artificial cloud (solid curve) compared with a best-fitted Gaussian density distribution (dashed curve) representing qualitatively the light energy deposited on the film during a time interval equal to the exposure time of the film.

In a good approximation, the total light energy deposited on the film is then given by (GOLOMB *et al.*, 1965):

$$H_t = \pi r_e^2 H(0) \qquad \text{(A.1)}$$

where $H(0)$ is the energy deposited in the center of the image and r_e is the Gaussian half-width i.e. the distance at which the radiant exposure is $1/e$ times the peak energy $H(0)$.

By means of an absolute calibration at 557.7 nm of the Kodak 2485 film giving the optical density versus radiance L (in $h\nu$ cm^{-2} sr^{-1}) and through the knowledge of the Gaussian radius r_e (in cm) and the exposure time (in s) the total light energy can easily be calculated:

$$H_t = \pi r_e^2 L(0)/t \quad (h\nu \text{ s}^{-1} \text{ sr}^{-1}). \qquad \text{(A.2)}$$

For a monochromatic light source emitting at 557.7 nm, relation (A.2) may also be written:

$$H_t(557.7) = 3.562 \times 10^{-19}\, \pi r_e^2 L(0)/t \quad (\text{J s}^{-1} \text{ sr}^{-1}). \qquad \text{(A.3)}$$

For the determination of the real total energy on the film in the case of a polychromatic light source, the spectral distribution of the light emitted by the artificial cloud, the relative spectral sensitivity of the film and the ratio of the real total energy to the energy deposited on the film in the case of a monochromatic light source have to be taken into account. The computations have been performed using a step-by-step conversion of the energy as a function of fixed wavelength intervals.

The wavelength range to be taken into consideration is limited, on one hand, by the relative sensitivity S of the Kodak 2485 film ($S = 0$ for $\lambda < 400$ nm and $\lambda > 700$ nm) and, on the other hand, by the luminous intensity E of the emitted NO—O spectrum representing a continuum ($E \approx 0$ for $\lambda < 400$ nm and $\lambda > 1.4$ μm). It is easy to see that the film used in our experiment is sensitive only to a fraction of the nitric oxide spectrum. The ratio of radiant power sensed by a 2475 film to the total radiant power emitted during a NO release is $\frac{1}{3}$ (GOOD, 1967). This value is also adopted for the 2485 film.

Finally the spectral range 400–700 nm has been divided into 13 intervals ($i = 1, \ldots, 13$) with a bandwidth $(\Delta\lambda)_i$ of 25 nm, except for the intervals 1 and 13 [bandwidth $(\Delta\lambda)_i = 12.5$ nm].

As already mentioned in Section 2.2 our calculations are based on previously determined spectra. The relative intensities were normalized to $E = 1$ at $\lambda = 550$ nm. By averaging the various sets of data a mean intensity distribution was obtained and the adopted constant values E_i represent the intensity of the mean curve in the center of each interval.

The relative spectral sensitivity of the 2485 film for the wavelength region of interest and for different optical densities has been measured and an average S_i factor was applied.

Taking into account the values of E_i and S_i, the ratio p of the real total energy to the energy deposited on the film in the case of a monochromatic light source emitting at $\lambda = 557.7$ nm can be calculated ($p = 0.83$).

Now equation (A.3) can be written as:

$$H_t = 3.562 \times 10^{-19} [p\pi r_e^2 L(0)/t](\pi D^2/4f^2) \quad (\mathrm{J\ s^{-1}}) \tag{A.4}$$

where D and f are respectively the lens diameter and the focal distance of the Gianini camera ($f/D = 0.87$).

The contribution of each wavelength interval i to the total energy deposited on the film is proportional to the ratio $P_i = E_i S_i / \Sigma E_i S_i$.

The energy H_i per wavelength interval is then:

$$H_i = 3.562 \times 10^{-19} [p\pi r_e^2 L(0)/t] \times (\pi D^2/4f^2) P_i \quad (\mathrm{J\ s^{-1}}). \tag{A.5}$$

This light energy can be converted into number of photons per second introducing a conversion factor ε_i.

Now we can write:

$$H_i = 3.562 \times 10^{-19} [p\pi r_e^2 L(0)/t] \times (\pi D^2/4f^2) P_i \varepsilon_i \quad (h\nu\ \mathrm{s^{-1}}). \tag{A.6}$$

The total quantity of light energy (H_t or $\sum H_i$) deposited on the film is only a fraction of the light energy emitted by the artificial clouds since during its transport it is attenuated by the atmospheric layers and by the camera lens. Furthermore, this energy is collected by a lens of area $\pi D^2/4$ at a slant path S_R from the nitric oxide release.

Taking into consideration all these factors we may write equation (A.6) in the following form:

$$H_i^* = 3.562 \times 10^{-19} [p\pi r_e^2 L(0)/t] \times (\pi D^2/4f^2)(16\pi S_R^2/\pi D^2) \times [P_i \varepsilon_i / T(A)_i T(G)_i] \quad (h\nu\ \mathrm{s^{-1}}) \tag{A.7}$$

where:

$T(A)_i = \exp(-\tau \sec Z)$ is the atmospheric transmission coefficient, τ_i is the total optical attenuation coefficient (ELTERMAN, 1964, 1968), Z is the zenith distance from the artificial cloud, $T(G)_i$ is the camera lens transmission coefficient (experimentally determined).

The asterisk points out that the energy relates to the artificial cloud.

The ratio of the radiant power sensed by the film to the total radiant power emitted during the release being $\frac{1}{3}$ we obtain:

$$H_t^* = 3 \sum_{i=1}^{13} H_i^*. \tag{A.8}$$

Thus the total number of photons emitted per second and per cubic centimeter amounts to:

$$I = H_t^*/(4\pi R^3/3) \quad (h\nu\ \mathrm{cm^{-3}\ s^{-1}}) \tag{A.9}$$

where R is the real mean radius of the artificial cloud.

Using the shorthand notation $V = 4\pi R^3/3$ and introducing the numerical values for p, D and f, (A.9) finally yields:

$$I = 5.907 \times 10^{-19} [r_e^2 L(0) S_R^2 / Vt] \times \sum_{i=1}^{13} [P_i \varepsilon_i / T(A)_i T(G)_i] \quad (h\nu\ \mathrm{cm^{-3}\ s^{-1}}). \tag{A.10) or (7}$$